Relaxation dynamics of charge patches formed inside an insulating capillary by ion impact

Eric Giglio, K. Tőkési, R.D. Dubois

Relaxation dynamics of charge patches formed inside an insulating capillary by ion impact

E. Giglio[1], K. Tőkési[2,3] and R. D. DuBois[4]

[1]*Centre de Recherche sur les Ions, les Matériaux et la Photonique (CIMAP), Normandie Univ, ENSICAEN, UNICAEN, CEA, CNRS, 14000 Caen, France, EU*

[2]*Institute for Nuclear Research, Hungarian Academy of Sciences (ATOMKI), Hungary, EU*
[3]*ELI-ALPS, ELI-HU Non-profit Kft., Dugonics tér 13, H-6720 Szeged, Hungary, EU*

[4]*Missouri University of Science and Technology, Rolla MO 65409 USA*

Abstract

The dynamics of the charge distribution produced at the inner surface of an insulating capillary by low energy ion impact are investigated theoretically in the case when the entrance, exit and outer capillary surface are grounded. Starting with the surface continuity equation, that describes the charge dynamics at the inner surface, we deduced an analytical solution of the continuity equation in the form of a linear combination of surface charge moments that satisfy the corresponding boundary conditions. We determined the relaxation rate of each moment, which is given as a function of the dimensions and electrical properties of the capillary. We found an approximate expression of the time evolution of the electric potential and field generated by a charge patch during and after beam irradiation. The time evolution of the total charge is also described in detail. Our findings are illustrated with examples.

Keywords: capillary, insulator, charge relaxation, surface charge dynamics, multipole expansion

Introduction

Under charged particle impact, insulator surfaces accumulate electric charges. The latter generate an electric field that, if sufficiently strong, prevents the following beam particles from hitting the insulator surface. Ion beam transmission through insulating capillaries and their surprising guiding power has been intensively studied since its discovery by Stolterfoht *et al*. [1] for nano-capillaries and by Ikeda *et al.* [2] for macroscopic glass capillaries. The injected ions are guided by the self-organized formation of charge patches at the inner capillary walls. As a result, slow ions can pass through insulator capillaries, even when the geometrical conditions do not allow it. Experimental and theoretical studies of this topic have been summarized in three review articles [3-5]. While the guiding of ions by charged patches is qualitatively understood, the complex nature of the electric conduction in such insulators makes quantitative predictions still a challenging task. Indeed, for a given ion beam, the guiding is entirely determined by the dynamics of the charge patches at the surface, which in turn depend (i) on the electrical properties of insulators under ion beam irradiation and (ii) on the position and geometry of grounded electrodes. In order to get some insights into the discharge dynamics of formerly created charged patches, a theoretical study of the charge relaxation in a glass tube is performed. For a capillary, tilted with respect to the beam axis, the beam generates one or several charge patches at various places at the inner capillary surface wall. If the injected beam

is blocked, the deposited charge patches relax due to conductivity of the insulator. We propose in this work to study the charge relaxation of injected charges patches during and after beam irradiation in the case of a glass tube capillary of large aspect ratio and where the entrance, the outlet and the outer surface are grounded. We give an analytical solution of the continuity equation in the form of a linear combination of surface charge moments that satisfy the corresponding boundary conditions. We deduce from the boundary conditions a general expression of the electric potential in the capillary as well as the guiding electric field. We also give the discharge of the total accumulated charge in the capillary. Finally, we illustrate the finding for the glass tube used in an experimental setup that will be described in a subsequent paper. We would like to mention that while the development in the manuscript has been done for a cylindrical shaped capillary, it can also be extended to conical shaped capillaries, which is another interesting class of capillaries.

Surface charge dynamics

We consider a cylindrically shaped glass capillary of length H, with an inner radius R_1, an outer radius of R_2 and which has a dielectric constant ε_r (see Fig.1). The entrance and the outer surface of the capillary are electrically grounded. The underlying model considers two interfaces namely the inner glass-vacuum interface of the capillary and the outer glass-metal interface. We assume here that each projectile of charge $+q$ that hits the surface, injects exactly q holes at the impact point, which are immediately trapped by hole-centers at the inner surface. We thus implicitly assume that the secondary electrons, emitted from the impact point, fall back to the impact point except for q electrons, which are picked up by the projectile [6]. In alkali glasses, the mobility of holes, electrons and anions is negligible compared to the mobility of alkali cations and the bulk conductivity κ_b in those glasses is dominated by the mobile cations. We further assume that the rate τ_h^{-1} at which the injected holes migrate into the bulk is negligible compared to the charge relaxation rate due to bulk conductivity, $\tau_h^{-1} \ll \tau_b^{-1} = \frac{\kappa_b}{\varepsilon_0 \varepsilon_r}$. This implies that the charge accumulates only at the inner surface and not in the bulk and can thus be represented by a surface charge density σ [7]. Consequently, the mobile ions are driven by a divergence-free (solenoidal) electric field $\vec{\nabla} \cdot \vec{E} = 0$ through the glass bulk. They can however accumulate or deplete at the interfaces. The dynamics of the surface charge density at the inner interface is given by the surface continuity equation,

$$\frac{\partial \sigma(\vec{s},t)}{\partial t} = -\kappa_b E_r(\vec{s},t) - \frac{\partial}{\partial z}[\kappa_s E_z(\vec{s},t)] - \frac{1}{R_1}\frac{\partial}{\partial \theta}[\kappa_s E_\theta(\vec{s},t)] + \gamma(\vec{s},t) I_{\text{inj}} \qquad (1)$$

where all quantities are taken at the inner surface, $\vec{s} = (R_1, \theta, z)$. The first right hand term, which is proportional to the bulk conductivity κ_b, stands for the mobile charge carriers that are driven from the inner to the grounded outer surface by the radial component E_r of the electric field. The second and third right hand terms stand for the charge carriers that are field driven at the inner interface respectively along the symmetry axis by the tangential field E_z and along the angular direction by the tangential field E_θ. The surface current is proportional to the surface conductivity κ_s. The last term represents the injected charge per unit time and unit area, with I_{inj} being the beam current and γ the hole injection cross-section. The electric field $\vec{E}(\vec{r},t) = -\vec{\nabla} V(\vec{r},t)$ that guides the ions and drives the deposited surface charge density $\sigma(\vec{s},t)$ away from the production region is deduced from the potential

$$V(\vec{r},t) = \int_{S_1} \frac{(\sigma + \sigma^p) ds_1}{4\pi\varepsilon_0 \, |\vec{r} - \vec{s}_1|} + \int_{S_2} \frac{\sigma^f \, ds_2}{4\pi\varepsilon_0 \, |\vec{r} - \vec{s}_2|} \qquad (2)$$

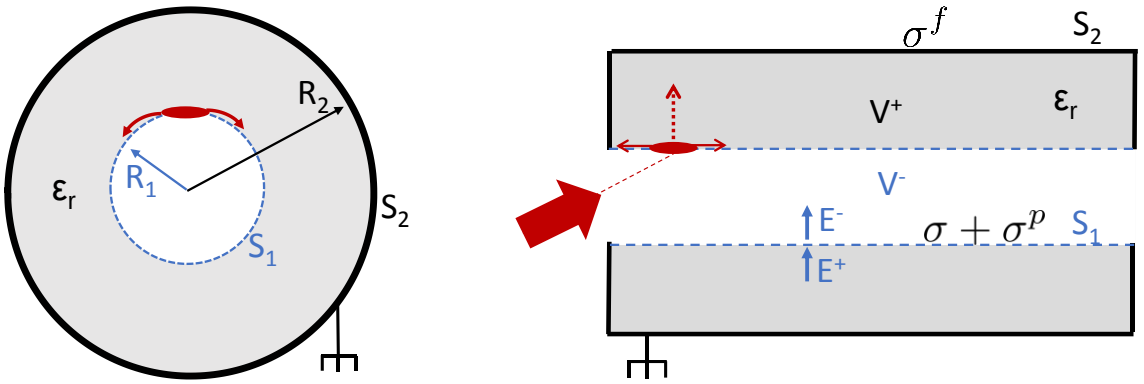

Figure 1: Scheme of the capillary. The outer surface S_2 is grounded. The insulating inner surface S_1 carries the accumulated surface charge density σ. The induced polarization charges σ^p and free charges σ^f are also shown. The tilted injected beam (large red arrow) deposits a charge patch near the entrance, which will relax in time due to a surface current along the angular direction (red arrows in left figure) a surface current along the axial direction and current through the bulk to the outer grounded surface (red arrows in right figure).

where σ^p stands for the bounded (polarization) surface charges at the inner glass-vacuum interface (S_1)and σ^f for the induced free charges at the conducting outer surface (S_2). The induced bound polarization charges σ^p at the inner interface are obtained by satisfying the jump condition of the electric field through the interface separating two dielectric media, with R_1^+ and R_1^- being the respectively the outer and inner region at the interface S_1,

$$\varepsilon_r E_r(r = R_1^+) - E_r(r = R_1^-) = \frac{\sigma}{\epsilon_0} \quad . \quad (3)$$

The induced free surface charges σ^f at the outer glass-metal interface surrounding the capillary (also referred to as image charges) are deduced by satisfying the boundary conditions, i.e. the potential is zero at the outer surface,

$$V(r = R_2) = 0 \quad . \quad (4)$$

Multipole expansion

To solve the continuity equation (1), we use a multipole expansion of the quantities involved in (1). The electric field being divergence-free means that the potential satisfies the Laplace equation with the boundary conditions given by (3) and (4). Also, the entrance and outlet being grounded, the potential is zero at the entrance, $V(r,\theta,0) = 0$ and at the outlet $V(r,\theta,H) = 0$. The latter conditions allow for a simple expansion of the potential by discretizing the wave number $k_n = n\,\pi/H$, with $n > 0$. The symmetry axis of the beam and of the tilted capillary define the x0z plane. The potential is assumed symmetric with respect to the x0z plane, so that $V(r,\theta,z) = V(r,-\theta,z)$. The expansion of the potential on harmonic functions differs depending on the domain. The function V^- represents the

potential for the inner domain ($0 \le r \le R_1$) and V^+ the potential for the domain ($R_1 \le r \le R_2$), with the continuity condition $V^-(R_1, \theta, z) = V^+(R_1, \theta, z)$,

$$V^-(r,\theta,z,t) = \sum_{m,n} v_{m,n}(t) \frac{I_m(k_n r)}{I_m(k_n R_1)} \cos(m\theta) \sin(k_n z) \quad , 0 \le r \le R_1 \quad (5a)$$

$$V^+(r,\theta,z,t) = \sum_{m,n} v_{m,n}(t) h_{mn}(r) \cos(m\theta) \sin(k_n z) \quad , \quad R_1 \le r \le R_2 \qquad (5b)$$

Where we introduced the auxiliary function $h_{mn}(r)$ defined as

$$h_{mn}(r) = \frac{I_m(k_n r)K_m(k_n R_2) - I_m(k_n R_2)K_m(k_n r)}{I_m(k_n R_1)K_m(k_n R_2) - I_m(k_n R_2)K_m(k_n R_1)} \quad ,$$

in order to simplify the notations, with $I_m(k_n r)$ and $K_m(k_n r)$ being modified Bessel functions of the first and second kind order m. Similar, we expand the surface density and injection cross section defined on the interface S_1, using the same basis as for the potential. Indeed, the grounded inlet and outlet imply that the surface density and source term are also zero at $z = 0$ and $z = H$,

$$\sigma(\theta,z,t) = \sum_{m,n} \sigma_{m,n}(t) \cos(m\theta) \sin(k_n z) \quad (5c)$$

$$\gamma(\theta,z,t) = \sum_{m,n} \gamma_{m,n}(t) \cos(m\theta) \sin(k_n z) \quad (5d)$$

Injecting equations (5a – 5d) into (1) yields an equation for each moment (*m*,*n*) of the expansion,

$$\frac{\partial \sigma_{m,n}}{\partial t} = v_{m,n} \left(\kappa_b \, h'_{mn}(R_1) - \kappa_s \left(\frac{m^2}{R_1^2} + k_n^2 \right) \right) + \gamma_{m,n} I_{\text{inj}} \quad (6)$$

The primed quantities in (6) are first order derivatives with respect to the radial coordinate *r*, i.e. $I'_m(k_n r) = \frac{k_n}{2} \left(I_{m-1}(k_n r) + I_{m+1}(k_n r) \right)$ and $K'_m(k_n R_1) = -\frac{k_n}{2} \left(K_{m-1}(k_n r) + K(k_n r) \right)$. Using the boundary condition (3),

$$v_{m,n} \left(\varepsilon_r h'_{mn}(R_1) - \frac{I'_m(k_n R_1)}{I_m(k_n R_2)} \right) = -\frac{\sigma_{m,n}}{\varepsilon_0} \quad (7)$$

allows eliminating the potential moments $v_{m,n}$ in (6), giving a first order differential equation for the surface charge moments $\sigma_{m,n}(t)$

$$\frac{\partial \sigma_{m,n}}{\partial t} = -\sigma_{m,n}(t) \left(\frac{b_{m,n}}{\tau_b} + \frac{c_{m,n}}{\tau_s} \right) + \gamma_{m,n}(t) I_{\text{inj}} \quad (8)$$

where we have introduced the bulk relaxation rate $\tau_b^{-1} = \frac{\kappa_b}{\varepsilon_0 \varepsilon_r}$ and the surface relaxation rate $\tau_s^{-1} = \frac{\kappa_s}{\varepsilon_0 R_1}$ and the dimensionless factors $b_{m,n}$ and $c_{m,n}$ defined by

$$b_{m,n} = \frac{h'_{mn}(R_1)}{h'_{mn}(R_1) - \varepsilon_r^{-1} \frac{I'_m(k_n R_1)}{I_m(k_n R_2)}} \quad (9a)$$

$$c_{m,n} = \frac{-\frac{1}{R_1}(m^2 + k_n^2 R_1^2)}{\varepsilon_r h'_{mn}(R_1) - \frac{I'_m(k_n R_1)}{I_m(k_n R_2)}} \qquad (9b)$$

The factors $b_{m,n}$ and $c_{m,n}$ give respectively the strength of the bulk relaxation rate and surface relaxation rate for each moment $\sigma_{m,n}$. They depend on the dimensions of the capillary, and more precisely on the ratios R_1/H and R_2/H, as well as its dielectric constant. The general solution of equation (13) is given by the expression

$$\sigma_{m,n}(t) = \sigma_{m,n}(0) \exp\left(-t\left(\frac{b_{m,n}}{\tau_b} + \frac{c_{m,n}}{\tau_s}\right)\right) + I_{\text{inj}} \int_0^t \gamma_{m,n}(t') \exp\left((t'-t)\left(\frac{b_{m,n}}{\tau_b} + \frac{c_{m,n}}{\tau_s}\right)\right) dt' \quad (10)$$

Each moment has its proper decay rate $\frac{b_{m,n}}{\tau_b} + \frac{c_{m,n}}{\tau_s}$ and source term $I_{\text{inj}}\, \gamma_{m,n}(t)$. Finally, the dynamics of the surface charge density can be obtained by injecting (10) into the surface charge expansion (5c).

In a nutshell, we have solved equation (1) in the general case of a cylindrical capillary with grounded outer surface (including the entrance and the outlet). The dimensions of the capillary are explicitly taken into account by the factors $b_{m,n}$ and $c_{m,n}$. The solution is given as a linear combination of time dependent surface charge moments $\sigma_{m,n}(t)$.
From the above charge dynamics equation (10), we can evaluate the time evolution of the electric field as well as the time evolution of the total accumulated charge Q in the capillary.

Inner electric potential and field

The guiding power of insulating capillaries is due to the charge patch formation that guides the ions. A charge patch at the inner surface generates an electric field inside the capillary that deflects/guides the injected ion beam. Using relation (7) that links the surface charge moment to the potential moments, we obtain the time-dependent potential inside the capillary as a linear combination of the time-dependent surface charge moments $\sigma_{m,n}(t)$,

$$V^-(r,\theta,z,t) = \sum_{m,n} \frac{\sigma_{m,n}(t)}{\varepsilon_0} a_{m,n} \frac{I_m(k_n r)}{I_m(k_n R_1)} \cos(m\theta) \sin(k_n z) \quad , 0 \le r \le R_1 \ , \quad (11)$$

with the dimensionless coefficients $a_{m,n}$ defined by (12). The latter give the "intensity" of the potential field generated by each surface charge moment.

$$a_{m,n} = \frac{1}{\varepsilon_r h'_{mn}(R_1) - \frac{I'_m(k_n R_1)}{I_m(k_n R_2)}} \quad (12)$$

The time-dependent inner electric field is simply given by the gradient of the inner potential $\overrightarrow{E^-}(\vec{r},t) = -\vec{\nabla}\, V^-$. For example, let $\vec{s}_p = \left(r = R_1^-, \theta = 0, z = z_p\right)$ be vector pointing at the center of a charge patch located at the inner surface. The time-dependent inner electric field normal to the surface (radial component) at position $\vec{s}_p$ is given by,

$$E_r^-\left(\vec{s}_p\right) = \sum_{m\geq 0}\sum_{n>0} a'_{m,n}\frac{\sigma_{m,n}(t)}{\varepsilon_0}\sin\left(k_n z_p\right) \quad , \qquad r < R_1 \quad (13)$$

with the dimensionless coefficients

$$a'_{m,n} = a_{m,n}\frac{I'_m(k_n R_1)}{I_m(k_n R_1)}$$

giving the intensity of the inner electric field for each surface charge moment. Again, the dimensions and dielectric constant of the capillary are "hidden" in the coefficients $a_{m,n}$ and $a'_{m,n}$.

Total charge

We may now turn to the evaluation of the total accumulated charge in the capillary. Integrating the surface charge density over the surface S_1, yields the time evolution of the total charge,

$$\begin{aligned} Q(t) &= \int_0^H dz \int_{-\pi}^{\pi} \sigma(\theta,z,t) R_1 d\theta = 2\pi R_1 H \sum_{n>0} \frac{\sigma_{0,n}(t)}{n}\frac{1-\cos(n\pi)}{\pi} \\ &= 4R_1 H \sum_{n>0,\ \text{odd}} \frac{\sigma_{0,n}(t)}{n} \end{aligned} \quad (14a)$$

Using the explicit expression of the surface charge moments $\sigma_{0,n}(t)$ yields the general expression of the time evolution of the total charge in the capillary in the presence of a source term.

$$Q(t) = \sum_{n>0,\ \text{odd}} \frac{q_{0,n}(0)}{n}\exp\left(-t\left(\frac{1}{\tau_b}+\frac{c_{0,n}}{\tau_s}\right)\right) + I_{\text{inj}}\int_0^t \frac{\Gamma_{0,n}(t')}{n}\exp\left(-t'\left(\frac{1}{\tau_b}+\frac{c_{0,n}}{\tau_s}\right)\right) dt' \quad (14b)$$

For simplicity, we introduced in (14b) the initial charge moment $q_{0,n}(0) = 4R_1 H\, \sigma_{0,n}(0)$ and probability $\Gamma_{0,n}(t) = 4R_1 H\, \gamma_{0,n}(t)$. Only angular moment $m = 0$ and wave numbers k_n with odd integer n contribute to the total charge. The selection rule on the integer n is due to our boundary condition, i.e. the outlet is grounded. Relaxing the constraint would imply a continuously varying k and remove the selection rule as kH/π would not necessarily be an integer any more. We also note that the weight of the charge moments decrease inversely proportional with *n*. For smooth patches the contribution of the higher modes to the total charge becomes negligible.

Application to a borosilicate glass tube

We illustrate the theoretical development with an example. In the following we consider the case of a borosilicate capillary with the dimension like the one used in our experimental setup. The borosilicate capillary is *H*=43 mm long with an inner radius $R_1 = 0.29$ mm, an outer radius of $R_2 = 2.75$ mm and has a dielectric constant $\varepsilon_r = 4.6$. Note the large difference in the ratios $R_1/H \ll R_2/H$. We assume in the following that the variation of the charge distribution along the *z*-axis is

sufficiently smooth within a step of 1 mm, so that the expansion in (10a-10d) can be limited to the integer $N = \text{Int}\left(\frac{H}{1}\right) = 43$ and only wave numbers, $k_{n\leq N}$, are considered. Further we assume that the charge distribution of a patch is well described by the first three angular moments, $(m \leq 2)$, namely the monopole, the dipole and the quadrupole angular moment. Note that the angular octupole moment $(m = 3)$ can be added easily, if needed. The factors $a_{m,n}$ $b_{m,n}$ and $c_{m,n}$ and can now be evaluated and a selection of the factors for $n \leq N$ and $m \leq 2$ is given in the table 1. Additionally, the relative variation of the factors as a function of $n < N$ is shown in figure 2.

Table 1: A selection of factors $\boldsymbol{b_{m,n}}$ and $\boldsymbol{c_{m,n}}$, giving respectively the strength of the bulk and surface relaxation rate for each moment $\boldsymbol{\sigma_{m\leq N,n\leq 2}}$. The coefficients $\boldsymbol{a'_{m,n}}$ give the ratio between the surface charge moment and the associated inner electric field

n	$\boldsymbol{a'_{0,n}}$	$\boldsymbol{a'_{1,n}}$	$\boldsymbol{a'_{2,n}}$	$\boldsymbol{b_{0,n}}$	$\boldsymbol{b_{1,n}}$	$\boldsymbol{b_{2,n}}$	$\boldsymbol{c_{0,n}}$	$\boldsymbol{c_{1,n}}$	$\boldsymbol{c_{2,n}}$
40	0.03	0.151	0.173	0.97	0.847	0.826	0.061	0.18	0.362
30	0.02	0.158	0.175	0.98	0.841	0.824	0.042	0.176	0.359
20	0.01	0.165	0.177	0.988	0.834	0.823	0.023	0.174	0.358
10	0.004	0.173	0.178	0.996	0.826	0.821	0.008	0.175	0.357
5	0.001	0.175	0.178	0.999	0.824	0.821	0.002	0.176	0.357
1	10^{-5}	0.176	0.178	0.9999	0.823	0.821	0.0001	0.176	0.357

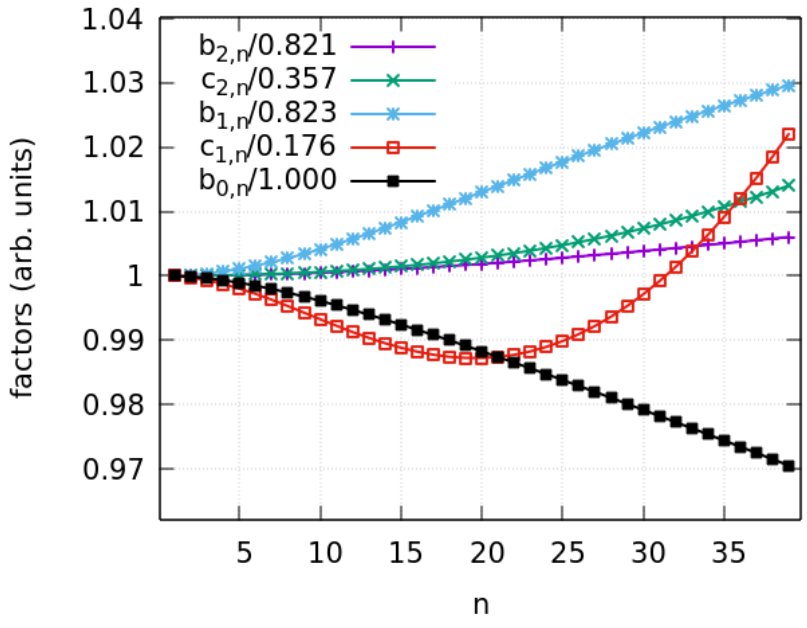

Figure 2: Relative variation of the factors as a function of n

The electric field generated by the monopole moments $\sigma_{0,n\leq N}$ is weak compared to the one generated by the dipole $\sigma_{1,n\leq N}$ and quadrupole moments $\sigma_{2,n\leq N}$, as can be seen from the factors $a_{m,n}$ in table 1. Indeed, for a given integer n, the coefficients $a_{0,n\leq N}$ of monopole term are at least 5 times smaller than those of the dipole and quadrupole term, $a_{0,n\leq N} \ll a_{1,n<N} \simeq a_{2,n\leq N}$ so that the monopole terms

can be neglected in the evaluation of the inner electric field. The time evolution of the field below the charge patch ($\vec{r} = \vec{s}_p$) is then given by

$$E_r\left(R_1^-, 0, z_p, t\right) \simeq \sum_{n>0}^{N} \left[a'_{1,n} \frac{\sigma_{1,n}(t)}{\varepsilon_0} + a'_{2,n} \frac{\sigma_{2,n}(t)}{\varepsilon_0} \right] \sin\left(k_n z_p\right) \quad (15)$$

Table 1 and figure 2 show that the factors $b_{1,n\leq N}$, $c_{1,n\leq N}$, $b_{2,n\leq N}$ and $c_{2,n\leq N}$ vary by less than 3% when *n* goes from 1 to *N=43*, so that they can be considered constant over that range. Hence, introducing the dipole and quadrupole relaxation rates,

$$\frac{1}{\tau_1} = \frac{0.83}{\tau_b} + \frac{0.17}{\tau_s}$$
$$\frac{1}{\tau_2} = \frac{0.83}{\tau_b} + \frac{0.36}{\tau_s}$$

the dynamics of the dipole and quadrupole moments can be approached by

$$\sigma_{1,n\leq N}(t) = \sigma_{1,n\leq N}(0) e^{-t/\tau_1} + I_{\text{inj}} \int_0^t \gamma_{0,n\leq N}(t') e^{-(t'-t)/\tau_1} \, dt' \quad (16a)$$

$$\sigma_{2,n\leq N}(t) = \sigma_{2,n\leq N}(0) e^{-t/\tau_2} + I_{\text{inj}} \int_0^t \gamma_{2,n\leq N}(t') e^{-(t'-t)/\tau_2} \, dt' \quad (16b)$$

Injecting (16a) and (16b) into (15) gives an expression that approaches the time-evolution of the inner electric field,

$$E_r\left(R_1^-, 0, z_p, t\right) \simeq E_1 e^{-\frac{t}{\tau_1}} + E_2 e^{-\frac{t}{\tau_2}} + \frac{I_{\text{inj}}}{\varepsilon_0} \int_0^t J_1(t') e^{-(t'-t)/\tau_1} \, dt' + \frac{I_{\text{inj}}}{\varepsilon_0} \int_0^t J_2(t') e^{-(t'-t)/\tau_2} \, dt' \quad (17)$$

where

$$E_1\left(z_p\right) = \sum_{n>0}^{N} a'_{1,n} \, \sigma_{1,n}(0) \sin\left(k_n z_p\right)/\varepsilon_0 \quad (18a)$$

$$E_2\left(z_p\right) = \sum_{n>0}^{N} a'_{2,n} \, \sigma_{2,n}(0) \sin\left(k_n z_p\right)/\varepsilon_0 \quad (18b)$$

are the amplitudes of the dipole and quadrupole moment of the electric field at point $z = z_p$ and

$$J_1\left(z_p, t\right) = \sum_{n>0}^{N} a'_{1,n} \gamma_{1,n}(t) \quad (18c)$$

$$J_2\left(z_p, t\right) = \sum_{n>0}^{N} a'_{2,n} \gamma_{2,n}(t) \quad (18d)$$

the dipole and quadrupole injection cross section at the observation point $z = z_p$. In the case where no beam is injected, $J_1(t) = J_2(t) = 0$, the relaxation of the inner electric field simplifies to a sum of two exponential functions, corresponding to the dipole and quadrupole contribution.

$$E_r\left(R_1^-, 0, z_p, t\right) \simeq E_1 e^{-\frac{t}{\tau_1}} + E_2 e^{-\frac{t}{\tau_2}} \quad (19)$$

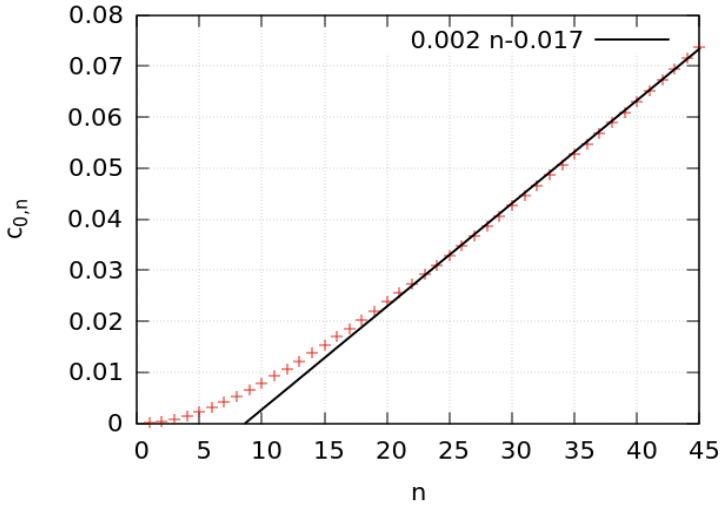

Figure 3: Dependence of the factors $c_{0,n}$ on the integer n

Expression (19) may be used to adjust the time-evolution of the force that deflects the ion beam. The advantage of using (19) as a fitting function of experimental data, is that it provides valuable information about the electrical conductivities of the insulating material.

We turn now to the expression of the time evolution of the total charge in the capillary. We note in figure 2 that the factors $b_{0,n\leq N} \simeq 1$ are close to unity, while we see in figure 3 that the factors $c_{0,n}$ are monotonically increasing with n, starting with $c_{0,0} = 0$. This differs from the $c_{1,n}$ and $c_{2,n}$ which are relatively constant. Also, the factors $c_{0,n\leq N}$ of the monopole moments are much lower than the factors $c_{1,n\leq N}$ of the dipole moment. The reason is that, for $m = 0$, one of the two surface relaxation channels becomes inactive, namely the one along the angular direction. The bulk relaxation channel dominates the surface relaxation channel for all modes $n \leq N$ if the following condition is satisfied,

$$c_{0,n\leq N} \ll \frac{\tau_s}{\tau_b} \xrightarrow{yields} \frac{b_{0,n\leq N}}{\tau_b} + \frac{c_{0,n\leq N}}{\tau_s} \simeq \frac{1}{\tau_b} \quad (20)$$

In that case, the time evolution of the total charge reads

$$Q(t) \simeq Q(0)\exp\left(-\frac{t}{\tau_b}\right) + \int_0^t I_{\text{dep}}(t')\exp\left(\frac{t'-t}{\tau_b}\right)dt' \quad (21)$$

where we introduced the total initial charge $Q(0) = \sum_{n>0,\,\text{odd}} q_{0,n}(0)/n$ and the deposited current $I_{\text{dep}}(t)$ defined as the difference between the injected and transmitted current,

$$I_{\text{inj}} - I_{\text{trans}}(t) = I_{\text{dep}}(t) = I_{\text{inj}} \int_0^H dz \int_{-\pi}^{\pi} \gamma(\theta, z, t) R_1 d\theta \quad (22)$$

For borosilicate glass, the typical bulk conductivity is about $\kappa_b \sim 1.5 \times 10^{-13}$ S/m at room temperature [8,9] yielding a bulk relaxation rate of about, $\tau_b^{-1} = 3.7$ mHz. The surface conductivity

in borosilicate is not a well-known quantity and depends strongly on the adsorbed impurities. At room temperature, it is typically less than 10^{-15} S in dry environment so that the surface relaxation rate is typically lower than 630 mHz ($\tau_s^{-1} \leq$ 630 mHz). Surface conductivity of Pyrex ® borosilicate glass plates have been recently measured by Gruber *et al.* [9], who found a surface conductivity of about $\kappa_s \sim 10^{-16}$ S. Assuming thus a bulk conductivity of $\kappa_b \sim 1.5 \times 10^{-13}$ S/m and surface conductivity $\kappa_s \sim 10^{-16}$ S, (yielding a surface relaxation rate of $\tau_s^{-1} = 63$ mHz) we see from table 1 that the condition (20) is only reasonably fulfilled for $n \leq n_c = 10$.

$$c_{0,n_c} = 0.008 \ll \frac{\tau_s}{\tau_b} = 0.06 \qquad (23a)$$

For $n \geq n_c$ the condition holds less and less, and the surface relaxation channel participates in a non-negligible way to the decay of the charge moments $q_{0,n>n_c}$. The trend of the factors $c_{0,n\leq N}$ is shown in figure 2. Note that the factors $c_{0,n}$ increase almost linearly for $n_c < n < N$ with the slope $\beta = 0.002$,

$$c_{0,n\geq n_c} \simeq \beta(n - n_c) \qquad (23b)$$

We will in the following try to give a general expression for decay of the initially accumulated charge in the absence of source term (no injected beam). Without losing any generality we can rewrite the decay of the accumulated charge using an auxiliary function $Q_c(t)$, which corresponds to the part of the charge that decays not only via the bulk channel but also via a non-negligible surface channel,

$$Q(t) \simeq \exp\left(-\frac{t}{\tau_b}\right)[Q(0) - Q_c(0) + Q_c(t\beta/\tau_s)] \quad (24)$$

with

$$Q_c(t\beta/\tau_s) = \sum_{n\geq n_c\,,\,\text{odd}} \frac{q_{0,n}(0)}{n} \exp\left(-t\frac{\beta(n-n_c)}{\tau_s}\right) \quad (25)$$

At this point, we have to make an assumption about the initial occupation numbers of the moments $q_{0,n}(0)$. We give here the example, where the initial occupation numbers of the charge moments decrease inversely proportional with $\geq n_c$,

$$q_{0,n\geq n_c}(0) \simeq \frac{q_{0,n_c}(0)}{n} \qquad (26)$$

In this particular case, the auxiliary function can be approached by

$$Q_c\left(\frac{t\beta}{\tau_s}\right) \simeq q_{0,n_c}(0) \sum_{n=n_c}^{\infty} \frac{e^{-t\beta(n-n_c)/\tau_s}}{n^2} = q_{0,n_c}(0) \sum_{0}^{\infty} \frac{\left(e^{-t\beta/\tau_s}\right)^n}{(n+n_c)^2} \qquad (27)$$

The last term in (27) has been rearranged to reveal the definition of the Lerch transcendent function $\phi(x, n_c, 2) = \sum_0^\infty x^n/(n+n_c)^2$. Noting that $Q_c(0) = q_{0,n_c}(0)\,\phi(1, n_c, 2)$, the auxiliary function may be expressed by

$$Q_c\left(\frac{t\beta}{\tau_s}\right) \simeq Q_c(0)\,\frac{\phi\left(e^{-t\beta/\tau_s}, n_c, 2\right)}{\phi(1, n_c, 2)} \qquad (28)$$

We obtain finally an approximated expression for the decay of the total charge,

$$Q(t) \simeq e^{-t/\tau_b}\left[\left(Q(0)-Q_c(0)\right)+Q_c(0)\,\frac{\phi\left(e^{-t\beta/\tau_s},n_c,2\right)}{\phi(1,n_c,2)}\right] \quad (29)$$

The quantity $Q(0)-Q_c(0)$ is the charge that decays purely via the bulk channel to the outer surface and $Q_c(0)$ the amount of charge located near the entrance and outlet and that decays via both channels, surface and bulk. In figure 4 we illustrate the influence of the surface decay channel on the total charge decay by showing normalized discharge curves for three different surface charge rates τ_s^{-1}, ranging from 0 to 630 mHz. We used $\beta = 0.002$, $n_c = 10$, and $\tau_b^{-1} = 3.7$ mHz. The percentage of the amount of charge that decays via both channels was fixed to $(Q_c(0)/Q(0) = 20\%)$. For $\tau_s^{-1} = 0$ mHz, the surface channel is deactivated and all the charge decays via the bulk channel. With increasing τ_s^{-1}, the initial decay is accelerated by the additional surface channel but tends then asymptotically to the bulk decay rate as the charge located near the grounded entrance and exit is removed. The effect becomes non-negligible for $\tau_s^{-1} \geq 630$ mHz.

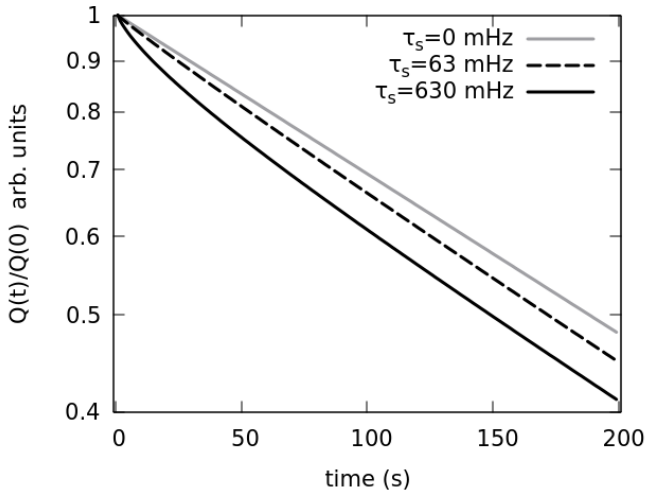

Figure 4: Discharge curves Q(t) for three different surface relaxation rates namely $\tau_s = 0$ (grey full line), $\tau_s = 63$ mHz (dashed black line), $\tau_s = 630$ mHz (black full line). The percentage of the amount of charge that decays via both channels was fixed to 20% $(Q_c(0)/Q(0) = 0.2)$.

The auxiliary function $Q_c(t)$ defined by (25) depends on charge occupation numbers $q_{0,n}(0)$. For a different law than (26), the auxiliary function $Q_c(t)$ will be modified accordingly. In this example, we used a glass capillary with the ratios $R_1/H \simeq 4 \times 10^{-3} \ll R_2/H \simeq 5 \times 10^{-2}$. Choosing a capillary with an outer radius R_2 of the order of R_1would significantly reduce the factors $c_{m,n}$ which are associated with the surface relaxation channel. Indeed, taking for example $R_2 = 0.3$ mm, would reduce by 70% the dipole and by 30% the quadrupole factors associated with the surface channel while increasing in (lower proportion) the factors $b_{m,n}$associated with the bulk channel. The development can also be applied to cylindrical shaped nano-capillaries in silicon sheets.

The idea was here to propose a general method for predicting the decay of the total charge as a function of the initial surface charge distribution. Expression (29) may be used, for example, to fit the decay of the total charge of a cylindrical capillary that was initially charged by a tilted ion beam as a non-negligible part of the charge is located near the grounded entrance. The charge decay deviates

from a purely exponential decrease, putting boundaries on the value of the surface conductivity of the insulator.

Conclusion:

We solved the surface charge continuity equation in the case of an insulating capillary tube with the outer surface, entrance and exit grounded. The analytical solution is given as a linear combination of surface charge moments that satisfy the corresponding boundary conditions. Each surface charge moment decays exponentially with a relaxation rate depending on its mode (m,k_n) and on the dimensions of the capillary. The analytical expression of the relaxation rate of each surface charge moment is given explicitly. Each relaxation rate includes contributions of the three possible relaxation channels, namely through the bulk, along the angular and along the axial direction at the surface. We showed that, depending on the mode (m,k_n), the relative importance of the three channels varies. We deduced from the boundary conditions the time evolution of the electric potential and electric field due to the charge patch produced by the injected ions at the inner capillary surface. The equations given in the text are of general scope and can be used to evaluate the charge dynamics in insulating capillaries of different dimensions and even in nano-capillaries of cylindrical shape. The method developed in the paper can also be extended to conical shaped capillaries, following the same approach. We illustrated our findings by an example that shows in particular how to use our solutions for the electric field and for the total charge to fit experimental data, allowing an easier interpretation of the experimental results.

Acknowledgements

This work was supported by PICS N° 245 358 Hongrie 2018 founding, by Hubert Curien (PHC) Balaton 2018 program, project number 40301VK and by the Bilateral relationships between France and Hungary in Science and Technology (S&T) under the project number 2017-2.2.5-TÉT-FR-2017-00008.

Bibliography

[1] N. Stolterfoht, J.-H. Bremer, V. Hoffmann, R. Hellhammer, D. Fink, A. Petrov and B. Sulik, Phys. Rev. Lett. **88** (2002) 133201

[2] T. Ikeda, K. Yasuyuki, T. M. Kojima, Y. Iwai, T. Kambara, Y. Yamazaki, M. Hoshino, T. Nebiki and T. Narusawa, Applied Phys. Lett. **89** (2006) 163502

[3] C. Lemell, J. Burgdörfer and F. Aumayr, *Progress in Surface Science* **88**, Issue 3 (2013) 237

[4] N. Stolterfoht, Y. Yamazaki, Physics Reports 629 (2016) 1–107

[5] T.M. Kojima, J. Phys. B: At. Mol. Opt. Phys. 51 (2018) 042001

[6] A. Cassimi, T. Ikeda, L. Maunoury, C. L. Zhou, S. Guillous, A. Mery, H. Lebius, A. Benyagoub, C. Grygiel, H. Khemliche, P. Roncin, H. Merabet, and J. A. Tanis, Phys. Rev. A **86** (2012) 062902.

[7] E. Giglio, R.D. DuBois, A. Cassimi and K.Tőkési, Nucl. Instr. and Meth. Phys. Res. B **354** (2015) 82

[8] M.M.R.A. Lima, R.C.C. Monteiro, M.P.F. Graça, M.G. Ferreira da Silva, Journal of Alloys and Compounds **538** (2012) 66

[9] E. Gruber, G. Kowarik, F. Ladening, J. P.Waclawek, F. Aumayr, R. J. Bereczky, K. Tőkési, P. Gunacker, T. Schweigler, C. Lemell and J. Burgdröfer, Phys. Rev. A **86** (2012) 062901